Acta Cryst E CRYSTALLOGRAPHIC COMMUNICATIONS

ISSN 2056-9890

Rietveld refinement of the langbeinite-type phosphate $K_2Ni_{0.5}Hf_{1.5}(PO_4)_3$

Liang Zhou,[a] Denys S. Butenko,[a] Ivan V. Ogorodnyk,[b] Nickolai I. Klyui[c] and Igor V. Zatovsky[a]*

[a]College of Physics, Jilin University 2699 Qianjin St., 130012 Changchun, People's Republic of China, [b]ShimUkraine LLC, 18, Chigorina Str., office 429, 01042 Kyiv, Ukraine, and [c]V. Lashkaryov Institute of Semiconductor Physics, NAS of Ukraine, 41 Pr. Nauki, 03028 Kyiv, Ukraine. *Correspondence e-mail: zvigo@yandex.ru

Received 4 August 2020
Accepted 1 September 2020

Edited by M. Weil, Vienna University of Technology, Austria

Keywords: powder diffraction; langbeinite structure type; multimetal phosphate; crystal structure.

CCDC reference: 2026681

Supporting information: this article has supporting information at journals.iucr.org/e

Polycrystalline potassium nickel(II) hafnium(IV) tris(orthophosphate), a langbeinite-type phosphate, was synthesized by a solid-state method and refers to langbeinite-type phosphates. The three-dimensional framework of the title compound is built up from two types of [MO_6] octahedra [the M sites are occupied by Hf:Ni in ratios of 0.754 (8):0.246 (8) and 0.746 (8):0.254 (8), respectively] and [PO_4] tetrahedra are connected *via* O vertices. The K^+ cations are located in two positions within large cavities of the framework, having coordination numbers of 9 and 12. The Hf, Ni and K sites lie on threefold rotation axes, while the P and O atoms are situated in general positions.

1. Chemical context

Langbeinite-related complex oxides have a variety of interesting properties, for example, ferroelectricity or ferroelasticity (Norberg, 2002). In particular, complex phosphates of this type have attracted attention for their high thermal and chemical stability, and many different combinations for structural substitutions are possible (Wulff *et al.*, 1992; Slobodyanik *et al.*, 2012). These characteristics made it possible to propose the family of langbeinite-type phosphates as successful hosts for the immobilization of radioactive waste (Orlova *et al.*, 2011). Moreover, in the last decade rare-earth (RE)-containing langbeinite-type phosphates have been studied intensively owing to their outstanding luminescent properties and applications in LEDs (Liang & Wang, 2011; Liu *et al.*, 2016; Sadhasivam *et al.*, 2017; Terebilenko *et al.*, 2020). Accordingly, further studies of iso- and heterovalent substitution within the cationic sites of the langbeinite structure are important. Structural data for langbeinite-type Hf-containing phosphates are scarce and include only $K_{1.93}Mn_{0.53}Hf_{1.47}(PO_4)_3$ (Ogorodnyk *et al.*, 2007*a*) and $K_2YHf(PO_4)_3$ (Ogorodnyk *et al.*, 2009).

In this report, we describe the powder X-ray refinement using the Rietveld method for the multimetal phosphate $K_2Ni_{0.5}Hf_{1.5}(PO_4)_3$ (**I**), structurally isotypic with the mineral langbeinite, $K_2Mg_2(SO_4)_3$ (Zemann & Zemann, 1957).

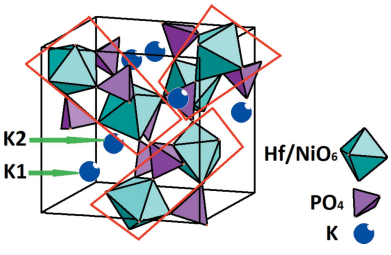

2. Structural commentary

As shown in Fig. 1, in the structure of (**I**) the K, Ni and Hf sites are localized on threefold rotation axes (Wyckoff position 4 *a*), while the P and all O atoms occupy general sites (12 *b*). Two metallic sites (Hf,Ni)1 and (Hf,Ni)2 show mixed occupancy

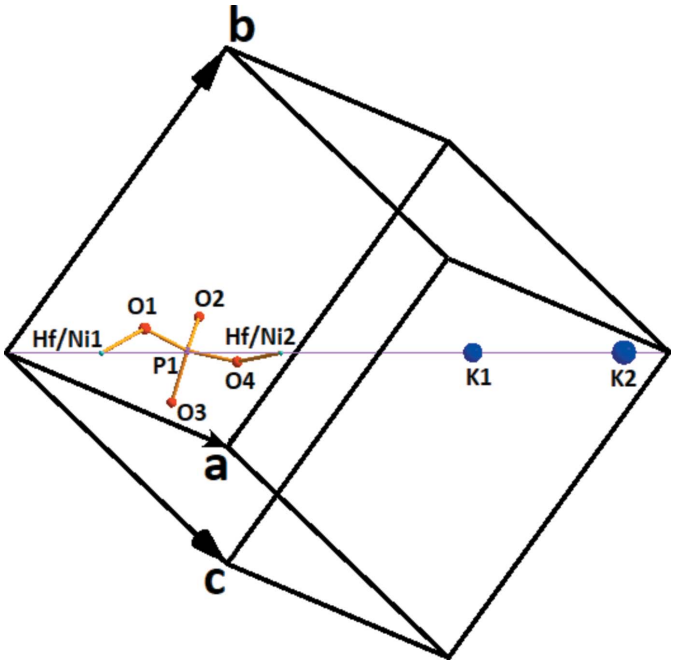

Figure 1
A view of the asymmetric unit of $K_2Ni_{0.5}Hf_{1.5}(PO_4)_3$, with displacement spheres drawn at the 50% probability level.

with a Hf:Ni ratio of about 0.75:0.25 (nickel proportion 0.246 (8) for the *M*1 site and 0.254 (8) for the *M*2 site). A similar M^{II}:M^{IV} ratio was also observed for isostructural phosphates of general composition $M^{I}M^{II}_{0.5}M^{IV}_{1.5}(PO_4)_3$, *viz*. $K_2Ni_{0.5}Ti_{1.5}(PO_4)_3$ (Ogorodnyk *et al.*, 2007*b*), $Rb_2Ni_{0.5}Ti_{1.5}(PO_4)_3$ (Strutynska *et al.*, 2015), $K_2Co_{0.5}Ti_{1.5}(PO_4)_3$ and $K_2Mn_{0.5}Ti_{1.5}(PO_4)_3$ (Ogorodnyk *et al.*, 2006), $K_2Ni_{0.5}Zr_{1.5}(PO_4)_3$ (Zatovsky, 2014), $K_{1.96}Mn_{0.57}Zr_{1.43}(PO_4)_3$ and $K_{1.93}Mn_{0.53}Hf_{1.47}(PO_4)_3$ (Ogorodnyk *et al.*, 2007*a*).

The (Hf,Ni)—O distances in (**I**) are 1.989 (15) and 2.121 (14) Å for the [(Hf,Ni)1O_6] octahedron, and 2.131 (17) and 2.172 (16) Å for the [(Hf,Ni)2O_6] octahedron. The two independent [(Hf,Ni)O_6] octahedra are linked by three [PO_4] tetrahedra to form an [$M_2P_3O_{18}$] building unit (Fig. 2). These building units are arranged along three directions (threefold rotation axes) and linked together *via* oxygen vertices, forming a three-dimensional framework structure. Pairs of K^+ cations (two independent sites) are localized in large cavities of the resulting framework. The potassium cations are found in 9- and 12-coordination by O atoms with K—O distances ranging from 2.854 (17) Å to 3.372 (18) Å (Table 1, Fig. 3), leading to distorted polyhedra. The [PO_4] tetrahedron shows considerable distortion (Table 1).

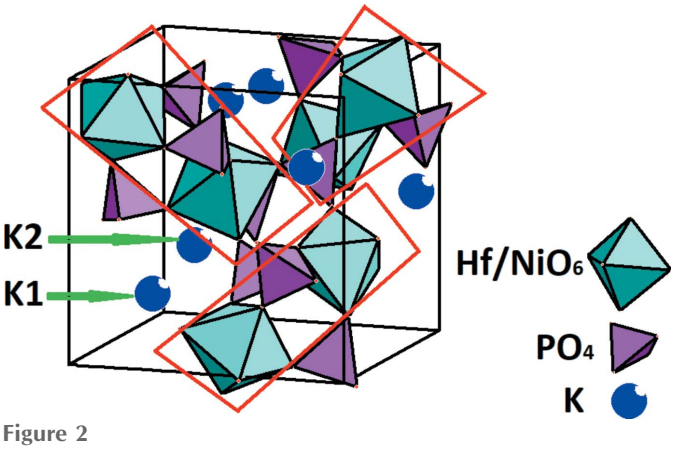

Figure 2
[$M_2P_3O_{18}$] building unit (highlighted in red frames) for (**I**). K^+ cations are shown as blue spheres of arbitrary radius.

Table 1
Selected geometric parameters (Å, °).

K1—O1^{i}	2.854 (17)	K2—O4^{iii}	3.372 (18)
K1—O4^{ii}	3.082 (17)	P1—O1	1.503 (15)
K1—O2^{ii}	3.103 (15)	P1—O2	1.533 (17)
K2—O3^{ii}	2.944 (16)	P1—O3	1.48 (2)
K2—O2^{iii}	2.987 (18)	P1—O4	1.506 (18)
K2—O4^{ii}	3.041 (18)		
O1—P1—O2	110.2 (10)	O2—P1—O3	112.6 (10)
O1—P1—O3	107.4 (10)	O2—P1—O4	106.0 (10)
O1—P1—O4	120.1 (10)	O3—P1—O4	100.3 (11)

Symmetry codes: (i) $-x+1, y+\frac{1}{2}, -z+\frac{1}{2}$; (ii) $-x+\frac{3}{2}, -y+1, z+\frac{1}{2}$; (iii) $-z+1, x+\frac{1}{2}, -y+\frac{3}{2}$.

For (**I**), the calculation of BVS (bond-valence sums) was performed using the parameters for Hf from Brese & O'Keeffe (1991), for Ni from Brown (private communication, 2001) and for K, P from Brown & Altermatt (1985). The corresponding occupation of the *M* sites by Hf and Ni atoms was taken into account. The sum of BVS of the cations is +23.67 valence units (v.u.), which is close to the −24 v.u. required for the O atoms.

3. Synthesis and crystallization

Compound (**I**) was synthesized using a solid-state reaction method. A well-ground starting mixture of 3.157 g HfO_2,

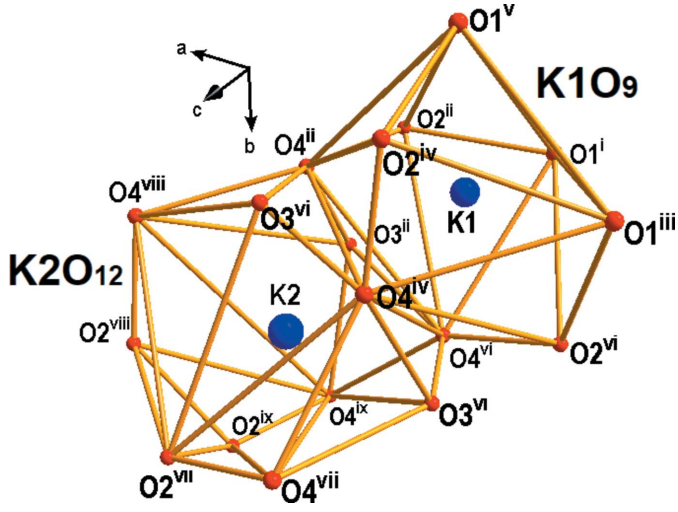

Figure 3
Coordination polyhedra [K1O_9] and [K2O_{12}] for (**I**). Displacement spheres are drawn at the 50% probability level. [Symmetry codes: (i) $-x+1, y+\frac{1}{2}, -z+\frac{1}{2}$; (ii) $-x+\frac{3}{2}, -y+1, z+\frac{1}{2}$; (iii) $-z+\frac{1}{2}, -x+1, y+\frac{1}{2}$; (iv) $-y+1, z+\frac{1}{2}, -x+\frac{3}{2}$; (v) $y+\frac{1}{2}, -z+\frac{1}{2}, -x+1$; (vi) $z+\frac{1}{2}, -x+\frac{3}{2}, -y+1$; (vii) $-z+1, x+\frac{1}{2}, -y+\frac{3}{2}$; (viii) $-y+\frac{3}{2}, -z+1, x+\frac{1}{2}$; (ix) $x+\frac{1}{2}, -y+\frac{3}{2}, -z+1$].

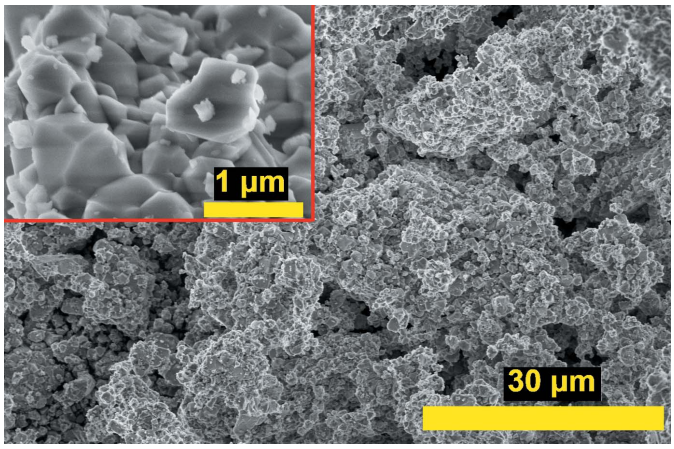

Figure 4
SEM image for (**I**) (Insert: image at higher magnification).

0.374 g NiO, 2.361 g KPO_3 and 1.150 g $NH_4H_2PO_4$ (molar ratio K:Ni:Hf:P = 4:1:3:6) was transferred to a ceramic crucible and pre-heated at 553 K for 2 h. The powder was re-ground, heated at 823 K for 3 h and then milled for 0.5 h in an agate mortar. The resulting fine powder was pressed into a pill and finally calcined at 1273 K for 100 h. The sample was ground before performing powder XRD data collection. Scanning electron microscopy (SEM, Magellan 400, recorded at 10 kV) showed that the obtained sample is an aggregate of small crystallites with a size less than 1 µm (Fig. 4).

4. Refinement

The experimental, calculated and difference pattern are shown in Fig. 5. Crystal data, data collection and structure refinement details are summarized in Table 2. Structure refinement was performed using $K_2YHf(PO_4)_3$ (Ogorodnyk *et al.*, 2009) as a starting model. A modified pseudo-Voigt function (Thompson *et al.*, 1987) was used for the profile refinement. The similar shape of the transition-metal octahedra indicated that both *M* positions are occupied by Ni and Hf simultaneously. For the refinement of their occupancies their coordinates and U_{iso} values were constrained together, and the sum of occupancies constrained to unity for both sites.

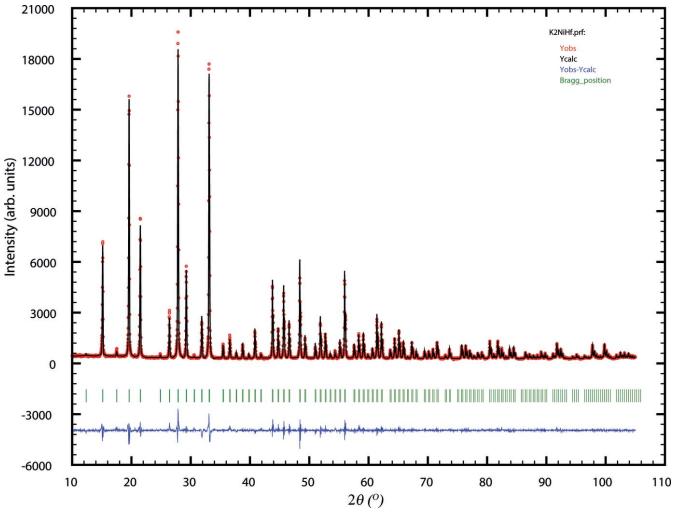

Figure 5
Rietveld refinement of $K_2Ni_{0.5}Hf_{1.5}(PO_4)_3$. Experimental (dots), calculated (red curve) and difference (blue curve) data for 2θ range 10–108°.

Table 2
Experimental details.

Crystal data	
Chemical formula	$K_2Ni_{0.5}Hf_{1.5}(PO_4)_3$
M_r	660.19
Crystal system, space group	Cubic, $P2_13$
Temperature (K)	293
a (Å)	10.12201 (5)
V (Å^3)	1037.05 (1)
Z	4
Radiation type	Cu $K\alpha_1$, λ = 1.540598 Å
Specimen shape, size (mm)	Flat sheet, 15 × 15
Data collection	
Diffractometer	Haoyuan Instrument Co. Ltd DX-2700B
Specimen mounting	Glass container
Data collection mode	Reflection
Scan method	Step
2θ values (°)	$2\theta_{min}$ = 10.008 $2\theta_{max}$ = 105.008 $2\theta_{step}$ = 0.020
Refinement	
R factors and goodness of fit	R_p = 6.111, R_{wp} = 7.831, R_{exp} = 4.020, R_{Bragg} = 4.709, $R(F)$ = 3.21, χ^2 = 4.410
No. of parameters	107
No. of restraints	3

Computer programs: data-collection and reduction software supplied by instrument manufacturer (http://www.haoyuanyiqi.com/en/xsxysy/s_23_30.html), *FULLPROF* (Rodriguez-Carvajal, 2020), *DIAMOND* (Brandenburg, 2006), *PLATON* (Spek, 2020), *WinGX* (Farrugia, 2012) and *enCIFer* (Allen *et al.*, 2004).

References

Allen, F. H., Johnson, O., Shields, G. P., Smith, B. R. & Towler, M. (2004). *J. Appl. Cryst.* **37**, 335–338.
Brandenburg, K. (2006). *DIAMOND*. Crystal Impact GbR, Bonn, Germany.
Brese, N. E. & O'Keeffe, M. (1991). *Acta Cryst.* B**47**, 192–197.
Brown, I. D. (2001). Private communication.
Brown, I. D. & Altermatt, D. (1985). *Acta Cryst.* B**41**, 244–247.
Farrugia, L. J. (2012). *J. Appl. Cryst.* **45**, 849–854.
Liang, W. & Wang, Y. (2011). *Mater. Chem. Phys.* **127**, 170–173.
Liu, J., Duan, X., Zhang, Y., Li, Z., Yu, F. & Jiang, H. (2016). *J. Alloys Compd.* **660**, 356–360.
Norberg, S. T. (2002). *Acta Cryst.* B**58**, 743–749.
Ogorodnyk, I. V., Zatovsky, I. V., Baumer, V. N., Slobodyanik, N. S., Shishkin, O. V. & Vorona, I. P. (2007*a*). *J. Solid State Chem.* **180**, 2838–2844.
Ogorodnyk, I. V., Zatovsky, I. V. & Slobodyanik, N. S. (2007*b*). *Russ. J. Inorg. Chem.* **52**, 121–125.
Ogorodnyk, I. V., Zatovsky, I. V. & Slobodyanik, N. S. (2009). *Acta Cryst.* E**65**, i63–i64.
Ogorodnyk, I. V., Zatovsky, I. V., Slobodyanik, N. S., Baumer, V. N. & Shishkin, O. V. (2006). *J. Solid State Chem.* **179**, 3461–3466.
Orlova, A. I., Koryttseva, A. K. & Loginova, E. E. (2011). *Radiochemistry*, **53**, 51–62.
Rodriguez-Carvajal, J. (2020). *FULLPROF*. Laboratoire Léon Brillouin (CEA–CNRS), France.

Sadhasivam, S., Manivel, P., Jeganathan, K., Jayasankar, C. K. & Rajesh, N. P. (2017). *Mater. Lett.* **188**, 399–402.
Slobodyanik, N. S., Terebilenko, K. V., Ogorodnyk, I. V., Zatovsky, I. V., Seredyuk, M., Baumer, V. N. & Gütlich, P. (2012). *Inorg. Chem.* **51**, 1380–1385.
Spek, A. L. (2020). *Acta Cryst.* E**76**, 1–11.
Strutynska, N. Yu., Bondarenko, M. A., Ogorodnyk, I. V., Zatovsky, I. V., Slobodyanik, N. S., Baumer, V. N. & Puzan, A. N. (2015). *Cryst. Res. Technol.* **50**, 549–555.
Terebilenko, K. V., Nedilko, S. G., Chornii, V. P., Prokopets, V. M., Slobodyanik, M. S. & Boyko, V. V. (2020). *RSC Adv.* **10**, 25763–25772.
Thompson, P., Cox, D. E. & Hastings, J. B. (1987). *J. Appl. Cryst.* **20**, 79–83.
Wulff, H., Guth, U. & Loescher, B. (1992). *Powder Diffr.* **7**, 103–106.
Zatovsky, I. V. (2014). *Acta Cryst.* E**70**, i41.
Zemann, A. & Zemann, J. (1957). *Acta Cryst.* **10**, 409–413.

supporting information

Acta Cryst. (2020). E**76**, 1634-1637 [https://doi.org/10.1107/S2056989020012062]

Rietveld refinement of the langbeinite-type phosphate $K_2Ni_{0.5}Hf_{1.5}(PO_4)_3$

Liang Zhou, Denys S. Butenko, Ivan V. Ogorodnyk, Nickolai I. Klyui and Igor V. Zatovsky

Computing details

Data collection: Software supplied by instrument manufacturer (http://www.haoyuanyiqi.com/en/xsxysy/s_23_30.html); cell refinement: *FULLPROF* (Rodriguez-Carvajal, 2020); data reduction: Software supplied by instrument manufacturer (http://www.haoyuanyiqi.com/en/xsxysy/s_23_30.html); program(s) used to solve structure: isomorphic replacement; program(s) used to refine structure: *FULLPROF* (Rodriguez-Carvajal, 2020); molecular graphics: *DIAMOND* (Brandenburg, 2006); software used to prepare material for publication: *PLATON* (Spek, 2020), *WinGX* (Farrugia, 2012) and *enCIFer* (Allen *et al.*, 2004).

(I)

Crystal data

$K_2Ni_{0.5}Hf_{1.5}(PO_4)_3$
M_r = 660.19
Cubic, $P2_13$
Hall symbol: P 2ac 2ab 3
a = 10.12201 (5) Å
V = 1037.05 (1) Å^3
Z = 4
D_x = 4.228 Mg m^{-3}

Cu $K\alpha$ radiation, λ = 1.540598 Å
T = 293 K
Particle morphology: tetrahedra
yellow
flat_sheet, 15 × 15 mm
Specimen preparation: Prepared at 293 K and 101.3 kPa

Data collection

Haoyuan Instrument Co. Ltd DX-2700B diffractometer
Radiation source: X-ray tube, X-ray
Graphite monochromator

Specimen mounting: glass container
Data collection mode: reflection
Scan method: step
$2\theta_{min}$ = 10.008°, $2\theta_{max}$ = 105.008°, $2\theta_{step}$ = 0.020°

Refinement

R_p = 6.111
R_{wp} = 7.831
R_{exp} = 4.020
R_{Bragg} = 4.709
$R(F)$ = 3.21
4751 data points
Profile function: Thompson-Cox-Hastings pseudo-Voigt * Axial divergence asymmetry
107 parameters

3 restraints
3 constraints
Standard least squares refinement
$(\Delta/\sigma)_{max}$ = 0.001
Background function: Linear Interpolation between a set background points with refinable heights
Preferred orientation correction: Modified March's Function

Fractional atomic coordinates and isotropic or equivalent isotropic displacement parameters (Å^2)

	x	*y*	*z*	U_{iso}*/U_{eq}	Occ. (<1)
K1	0.7042 (5)	0.7042 (5)	0.7042 (5)	0.028 (4)*	

K2	0.9319 (8)	0.9319 (8)	0.9319 (8)	0.044 (4)*	
Ni1	0.14423 (16)	0.14423 (16)	0.14423 (16)	0.0022 (12)*	0.246 (8)
Ni2	0.4147 (2)	0.4147 (2)	0.4147 (2)	0.0019 (12)*	0.254 (8)
Hf1	0.14423 (16)	0.14423 (16)	0.14423 (16)	0.0022 (12)*	0.754 (8)
Hf2	0.4147 (2)	0.4147 (2)	0.4147 (2)	0.0019 (12)*	0.746 (8)
P1	0.4624 (6)	0.2349 (10)	0.1229 (9)	0.004 (2)*	
O1	0.3218 (13)	0.2314 (17)	0.0752 (16)	0.011 (6)*	
O2	0.5508 (14)	0.3023 (16)	0.0201 (15)	0.008 (4)*	
O3	0.5028 (13)	0.0973 (17)	0.1500 (18)	0.008 (6)*	
O4	0.4953 (16)	0.2985 (17)	0.2533 (14)	0.009 (6)*	

Atomic displacement parameters (Å²)

	U^{11}	U^{22}	U^{33}	U^{12}	U^{13}	U^{23}
?	?	?	?	?	?	?

Geometric parameters (Å, º)

K1—O1^{i}	2.854 (17)	Hf1—O1	2.121 (14)
K1—O4^{ii}	3.082 (17)	Hf1—O2^{x}	1.989 (15)
K1—O2^{ii}	3.103 (15)	Hf1—O1^{xi}	2.121 (14)
K1—O1^{iii}	2.854 (17)	Hf1—O2^{xii}	1.989 (15)
K1—O4^{iv}	3.082 (17)	Hf2—O4	2.172 (16)
K1—O2^{iv}	3.103 (15)	Hf2—O3^{i}	2.131 (17)
K1—O1^{v}	2.854 (17)	Hf2—O4^{xi}	2.172 (16)
K1—O4^{vi}	3.082 (17)	Hf2—O3^{iii}	2.131 (17)
K1—O2^{vi}	3.103 (15)	Ni1—O1	2.121 (14)
K2—O3^{ii}	2.944 (16)	Ni1—O2^{x}	1.989 (15)
K2—O2^{vii}	2.987 (18)	Ni1—O1^{xi}	2.121 (14)
K2—O4^{ii}	3.041 (18)	Ni1—O2^{xii}	1.989 (15)
K2—O4^{vii}	3.372 (18)	Ni2—O4	2.172 (16)
K2—O3^{iv}	2.944 (16)	Ni2—O3^{i}	2.131 (17)
K2—O2^{viii}	2.987 (18)	Ni2—O4^{xi}	2.172 (16)
K2—O4^{iv}	3.041 (18)	Ni2—O3^{iii}	2.131 (17)
K2—O4^{viii}	3.372 (18)	P1—O1	1.503 (15)
K2—O3^{vi}	2.944 (16)	P1—O2	1.533 (17)
K2—O2^{ix}	2.987 (18)	P1—O3	1.48 (2)
K2—O4^{vi}	3.041 (18)	P1—O4	1.506 (18)
K2—O4^{ix}	3.372 (18)		

O1—Hf1—O2^{x}	90.8 (6)	O1^{xi}—Ni1—O2^{x}	87.8 (6)
O1—Hf1—O1^{xi}	93.7 (6)	O2^{x}—Ni1—O2^{xii}	87.7 (6)
O1—Hf1—O2^{xii}	175.2 (6)	O1^{xi}—Ni1—O2^{xii}	90.8 (6)
O1^{xi}—Hf1—O2^{x}	87.8 (6)	O3^{i}—Ni2—O4	95.2 (6)
O2^{x}—Hf1—O2^{xii}	87.7 (6)	O4—Ni2—O4^{xi}	94.5 (6)
O1^{xi}—Hf1—O2^{xii}	90.8 (6)	O3^{iii}—Ni2—O4	168.5 (6)
O3^{i}—Hf2—O4	95.2 (6)	O3^{i}—Ni2—O4^{xi}	78.6 (6)
O4—Hf2—O4^{xi}	94.5 (6)	O3^{i}—Ni2—O3^{iii}	92.7 (6)

O3^{iii}—Hf2—O4	168.5 (6)	O3^{iii}—Ni2—O4^{xi}	95.2 (6)
O3^{i}—Hf2—O4^{xi}	78.6 (6)	O1—P1—O2	110.2 (10)
O3^{i}—Hf2—O3^{iii}	92.7 (6)	O1—P1—O3	107.4 (10)
O3^{iii}—Hf2—O4^{xi}	95.2 (6)	O1—P1—O4	120.1 (10)
O1—Ni1—O2^{x}	90.8 (6)	O2—P1—O3	112.6 (10)
O1—Ni1—O1^{xi}	93.7 (6)	O2—P1—O4	106.0 (10)
O1—Ni1—O2^{xii}	175.2 (6)	O3—P1—O4	100.3 (11)

Symmetry codes: (i) −*x*+1, *y*+1/2, −*z*+1/2; (ii) −*x*+3/2, −*y*+1, *z*+1/2; (iii) −*z*+1/2, −*x*+1, *y*+1/2; (iv) −*y*+1, *z*+1/2, −*x*+3/2; (v) *y*+1/2, −*z*+1/2, −*x*+1; (vi) *z*+1/2, −*x*+3/2, −*y*+1; (vii) −*z*+1, *x*+1/2, −*y*+3/2; (viii) −*y*+3/2, −*z*+1, *x*+1/2; (ix) *x*+1/2, −*y*+3/2, −*z*+1; (x) *x*−1/2, −*y*+1/2, −*z*; (xi) *z*, *x*, *y*; (xii) −*z*, *x*−1/2, −*y*+1/2.